2012

A novel cantilever for bi-harmonic atomic force microscopy

Muthukumaran Loganathan

Department:

A NOVEL CANTILEVER FOR BI-HARMONIC ATOMIC FORCE MICROSCOPY

by

MUTHUKUMARAN LOGANATHAN

A THESIS

Presented to the Faculty of the Graduate School of the

MISSOURI UNIVERSITY OF SCIENCE AND TECHNOLOGY

In Partial Fulfillment of the Requirements for the Degree

MASTER OF SCIENCE IN MECHANICAL ENGINEERING

2012

Approved by

Douglas A. Bristow, Advisor
Robert G. Landers
Jagannathan Sarangapani

PUBLICATION THESIS OPTION

This thesis consists of two articles that have/will be published and has been prepared in the style recommended by the respective journal publication. Pages 6-23 have been published in the Review of Scientific Instruments journal. Pages 24-40 will be submitted for publication in the Nanotechnology journal. Appendix has been added for purposes normal to thesis/dissertation writing.

ABSTRACT

Tapping mode (TM) AFM is a popularly used AFM technique in which an oscillating sharp tip mounted on a micro cantilever is used to probe the surface of interest with nanoscale resolution by making intermittent (tapping) contact with the surface. Any change in surface profile affects the tip amplitude, and is detectable only if it results in an amplitude change that is significant enough to be measured by the laser detector. Hence, it is desirable to have a micro cantilever that is sensitive to surface changes so as to provide sharper images and better surface resolution.

In the first part of this thesis, a novel method to improve the measurement sensitivity of the cantilever has been proposed. In this method a driving signal composed of two harmonics is used to generate a tapping trajectory whose valley is broader compared to conventional sinusoidal trajectory. Such a trajectory reduces the velocity of tapping and allows the tip to spend more time in proximity to the sample. Numerical analysis indicates reduction in impact forces and improvement in measurement sensitivity. Experimental results demonstrate increase in image sharpness and reduction in tip wear.

In the second part of this thesis, a new cantilever design, called a “bi-harmonic” cantilever is presented. This cantilever design has a second resonant frequency twice its first resonant frequency, and can be fabricated from commercial cantilevers through silicon etching. Numerical results indicate this cantilever assists in obtaining better sensitivity using a smaller input drive force, compared to commercial cantilevers. Surface images obtained using bi-harmonic cantilevers exhibit improved surface tracking, and thus sharper imaging, which is a direct benefit of higher sensitivity.

ACKNOWLEDGMENTS

I would like to express my sincere gratitude to my advisor, Dr. Douglas Bristow, for his unwavering support and positive attitude towards my research work. Without his guidance and insights this work would not have materialized. I deeply appreciate his mentorship, constructive criticism, and funding that have made my graduate experience productive and memorable.

I would like to thank Dr. Robert Landers and Dr. Jagannathan Sarangapani for graciously accepting to be on my thesis committee. I would also like to thank Material Research Center at Missouri S&T for the funding and support offered to my research. I thank my fellow lab members of PMCL Santosh, Mark, Tong and Alireza for their support and encouragement. A special thanks to Alireza for engaging in long technical discussions and sharing his insights about the AFM.

On a personal note, I would like to thank my uncle and aunt, Mr. Ekambaram and Mrs. Hemavathi for raising me since I was a kid and molding me into what I am today. I thank my uncle, Mr. Theertheswaran for his affection and unflinching confidence in me. Last but not the least, I thank my parents, Loganathan and Anbalagi for their love and kindness.

TABLE OF CONTENTS

Page

LIST OF ILLUSTRATIONS

Figure Page

LIST OF TABLES

1. INTRODUCTION

Advancement in the field of nanotechnology can be attributed to the invention of state of the art tools that enable visualization and manipulation of nano structures with relative ease. The Atomic force microscope (AFM) is one of the foremost and versatile tool that is capable of measuring nano surfaces apart from nano manipulation, nano assembly, and nano lithography. The AFM comes under the classification of scanning probe microscopy, which is a technique that involves scanning the surface of interest with a sharp tip or probe.

The Atomic Force Microscope (AFM) was invented by Binnig et al. in 1986, and is capable of generating 3D plots of surface with a resolution in the order of nanometers. Unlike its predecessor, the scanning tunneling microscope, AFM can be used to image both conducting and non conducting surfaces. Moreover its ability to operate under ambient conditions makes it an apt tool to study biological samples at nano level. The integral part of the AFM is the nano sized tip mounted on one end of a micro cantilever that acts as sensor to detect surface characteristics. It is normally made of silicon, doped with traces of antimony, with the top face often coated with metal or metal oxides for enhanced laser reflection. This tip, when brought in close proximity the surface, experiences forces including short range repulsive forces, weak Van der Waal's attractive forces, capillary forces, adhesion, magnetic, electrostatic forces. Such forces affect the motion of the cantilever which is detected by shining a laser on the cantilever and monitoring the reflected beam using an optical detector. Among all the nano scale forces the repulsive forces and the Van der Waal's attractive forces are always present. The repulsive forces are strong force fields that span a region of 1 – 3 Angstroms above the

surface. The attractive forces are comparatively weak and span few nanometers based on the material of the surface.

Based on the way the tip probes the surface, the AFM can be operated in three different modes namely contact mode, non contact mode and tapping mode. The contact mode is the simplest of the operation in which a static probe is made to be in constant contact with the sample surface while the sample is moved in a raster scan pattern. In other words the probe remains the repulsive regime of the surface for the entire scan period. This is a closed loop process where the deflection of the cantilever is regulated by controlling the Z-stage on which the sample is placed as in Figure 1.1. Since the tip and the sample are in constant contact both suffer considerable wear.

The tip wear and sample damage can be greatly reduced by operating in non-contact mode. In this mode the cantilever is made to probe the attractive force regime of the surface. In other words the cantilever does not come in physical contact with the surface. A static probe has the possibility of getting pulled into the surface or drifting away from the sample it is made to oscillate near its resonance. Since the attractive forces are very small compared to the repulsive forces, very sensitive cantilever and high resolution laser detectors are required. A feedback control loop is required to regulate the amplitude and thus maintain a constant offset between tip and the sample.

The tapping mode is most widely used AFM technique where the oscillating micro cantilever is made to intermittently “tap” the surface. Unlike non contact mode, where the probe oscillates only in attractive region, the oscillating probe in tapping mode traverses both attractive and repulsive regime alternatively. The surface variation affects amplitude of the cantilever which is measured using a laser – detector pair. Tapping

mode is a feedback control process where the amplitude of the cantilever is regulated by controlling the z-piezo on which the sample rests. The change in amplitude is directly proportional to the change in surface height hence the corrective action (z-piezo displacement) taken to regulate the cantilever amplitude directly represents the surface variations.

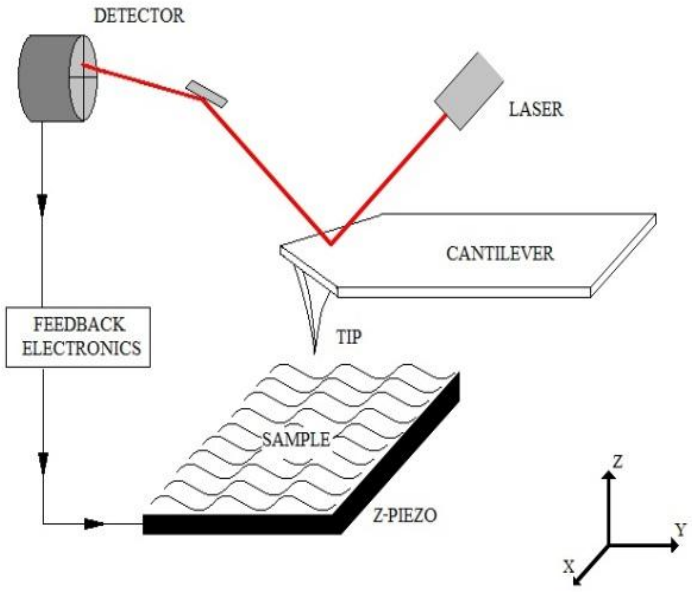

Figure 1.1 Schematic of an AFM

In Tapping mode AFM the ability to obtain good surface image depends on effectiveness of the control scheme, which depends on many factors including the signal-to-noise ratio. While many efforts have been made to improve the detection electronics to improve signal-to-noise ratio, the mechanical cantilever and probe are a critical element of the sensing. Cantilever research is primarily focused on fabricating the cantilever and variations in tip geometry and materials. There are also considerable efforts at AFM operation at near 0 Kelvin to minimize thermal noise. However, to date,

there has been little effort at improving the mechanical signal, that is, the sensitivity of the cantilever motion to change in response to a change in sample height. A high sensitivity means that a small change in surface height induces large change in the cantilever amplitude, which can more easily be detected by the controller. Hence high sensitivity enables good surface tracking, which will produce sharper images.

2. RESEARCH OBJECTIVE

Rapid development in the field of micro and nano scale engineering have posed ever increasing demand on developing powerful instruments for investigating features as small as atoms with precision. This involves improving the sensitivity of tools like the AFM. This thesis explores one of the ways to improve the measurement sensitivity of tapping mode (TM) atomic force microscopes. The method described involves reshaping the tapping trajectory of the tip so as to obtain better sensitivity. Though the technique has been developed for tapping mode AFM it can also be extended to non contact AFM.

PAPER

I. MEASUREMENT SENSITIVITY IMPROVEMENT IN TAPPING-MODE ATOMIC FORCE MICROSCOPY THROUGH BI-HARMONIC DRIVE SIGNAL

Muthukumaran Loganathan, Santosh R Kodandarama, and Douglas A Bristow

ABSTRACT

This article presents a novel method to improve the measurement sensitivity and reduce impact forces in tapping-mode atomic force microscopy by reshaping the tip trajectory. A tapping drive signal composed of two harmonics is used to generate an oscillating trajectory with a broader valley compared to the typical sinusoidal trajectory. The wide broad valley reduces the velocity of the tip in the vicinity of the sample and allots a greater portion of each period in the vicinity of the sample. Numerical simulations show that this results in decreased impact force and increased sensitivity of the cantilever oscillation to changes in tip-sample offset. Experimental results demonstrate an increase in image sharpness and decrease in tip wear using the bi-harmonic driving signal.

I. INTRODUCTION

The atomic force microscope (AFM) is one of the most versatile tools for surface analysis at the nanoscale[1]. In particular, the tapping mode AFM[2-3] is a widely used imaging technique. Tapping mode involves a periodic excitation of the cantilever probe such that it oscillates near resonance and intermittently “taps” on the sample. Compared

to other modes, tapping mode induces low tip-to-sample interaction forces and can be used to image a wide variety of materials, including soft samples. Research into the dynamics of the tapping mode over the past nearly 20 years has enhanced the capability and reliability of the tapping mode. Initially the Q-factor of the cantilever was a focus[4-6], as higher Q-factors result in higher force sensitivity, but also longer settling times, and thus slower imaging. Low noise deflection sensors and small amplitude tapping mode have demonstrated high measurement sensitivity in liquids[7-9]. At the same time, dynamic analysis provided new understanding of the process[10-11]. The analysis explains that image artifacts and instability are the result of multiple stable dynamic equilibria. In many cases, a change in process parameters such as tapping frequency or amplitude set point can eliminate the artifacts or restabilize the image[12]. Other control systems approaches have been proposed to expand the stable imaging range[13-14].

Recent efforts focus on measuring, or even exciting the cantilever, at multiple eigenmode frequencies of the cantilever. The additional information contained in the higher mode response is used to measure material properties, such as elastic modulus[15-16], and electrostatic forces[17-18]. When correlated with known material responses, the higher mode information can provide high resolutions maps of material composition[19-24].

In this article, we propose a new type of multi-frequency tapping mode. Here, additional frequencies are added at the higher harmonics of the fundamental drive signal, as opposed to previous works where the frequencies are at the higher eigenmode frequencies of the cantilever. The objective of our approach also differs. Rather than attempting to extract additional information from the sample, the multi-frequency tapping used here is intended to reshape the periodic tapping trajectory to one with more

favorable tapping dynamics. In principle, any periodic trajectory can be created using a sufficient number of harmonic frequencies, but for simplicity, we consider driving the cantilever with the first two harmonics. Through careful selection of the second harmonic parameters, the trajectory is reshaped to have a wider valley at the point of contact with the sample. As shown later in this article, the reshaped trajectory results in higher measurement sensitivity and lower interaction forces. The required instrument modification to obtain these results is minimal, as it requires only the connection of an arbitrary waveform function generator to the amplifier circuit for the tapping piezo in an off-the-shelf tapping-mode AFM. No change in sensing systems, electronics, or software is necessary to obtain the performance improvements.

II. MODEL DESCRIPTION

The dynamics of the AFM cantilever in air can be described as the spring-mass-damper system[12],

$$\ddot{x}(\tau)+\frac{\dot{x}}{Q}(\tau)+x(\tau)=\frac{F_{dr}(\tau)+F_{ts}(x)}{k}, \tag{1}$$

where x is the displacement of the tip from its equilibrium position, $\tau = t\omega_o$ is a scaled time, ω_o is the resonant frequency of the cantilever, Q is the quality factor of the cantilever, k is the cantilever spring constant, F_{dr} is the drive force and F_{ts} is the tip-sample interaction force. Several models have been proposed for the tip-sample interaction forces. Here we use the Lennard-Jones potential[25-27] which is given by,

$$\mathrm{F}_{ts}(x) = \frac{A_1 R}{180(x_s+x)^8}-\frac{A_2 R}{6(x_s+x)^2}, \tag{2}$$

where, A_1 and A_2 are the Hamaker constants for the repulsive and attractive potentials respectively, R is the probe tip radius and x_s is the distance between the cantilever equilibrium and sample. The drive force is typically a sinusoid,

$$F_{dr} = A\sin(\beta\tau), \tag{3}$$

where the amplitude, A, and frequency, $\beta = \omega/\omega_o$, are tuning parameters. Typically, β is selected to be 1 indicating the drive signal operates at the resonant frequency of the cantilever[12] and A is adjusted to regulate the tapping force.

It is well known that the forcing function (3) results in a sinusoidal free response, as illustrated in Figure 1. The amplitude A, frequency β, and offset x_s determine the magnitude of impact forces and the resolution of the image[28]. The critical portion of the trajectory is at the valley, where the cantilever probe interacts with the sample. Consider now the proposed broad-valley trajectory illustrated in Figure 1. The wider valley reduces the velocity as the probe nears the sample, which allows the probe to spend a greater portion of each period in the vicinity of the sample. One possible model for a broad-valley trajectory is,

$$x_{desired}(\tau) = A_0\left[\sin(\beta\tau) + \gamma\sin\left(2\beta\tau - \frac{\pi}{2}\right)\right], \tag{4}$$

whose second time-derivative at the valley is given by,

$$\ddot{x}_{desired}(\tau_{valley}) = A_0\beta^2(1-4\gamma). \tag{5}$$

From (5), it is clear that the width of the valley can be adjusted by $0\leq\gamma<0.25$. It can also be verified that for γ in this range $0\leq\gamma<0.25$, the peak-to-peak amplitude of the

trajectory is A_0. In order to generate the broad-valley trajectory, two harmonics are needed in the drive signal, as,

$$F_{dr} = A\left[\sin\left(\beta\tau + \varphi_1\right) + B\sin(2\beta\tau + \varphi_2)\right]. \tag{6}$$

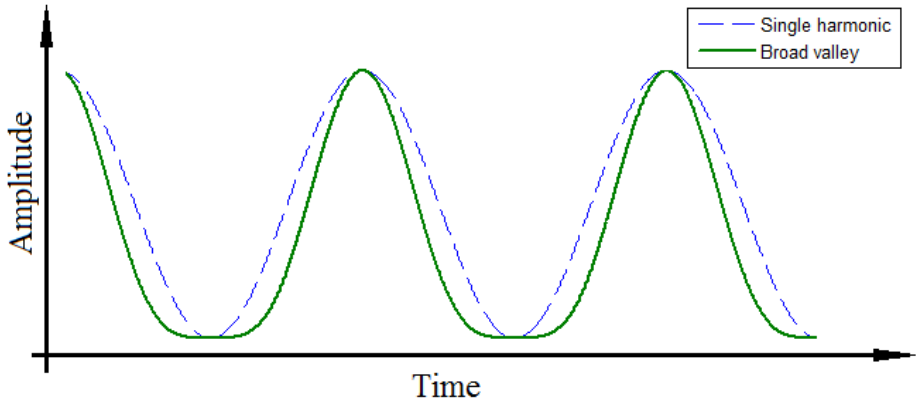

FIG. 1. Single harmonic and broad valley trajectories

The free response to the two-harmonic drive signal is obtained using standard Fourier analysis techniques as,

$$x(\tau) = \mathrm{A}\left|G(j\beta)\right|\sin\left(\beta\tau + \varphi_1 + \angle G(j\beta)\right) \; + \; AB\left|G(j2\beta)\right|\sin\left(2\beta\tau + \varphi_2 + \angle G(j2\beta)\right), \tag{7}$$

where G(jω) is the Fourier transform of the cantilever, (1). Comparing 7) to (4) and considering the resonance case (β=1), the broad-valley trajectory is obtained using the drive signal parameters,

$$A = A_0\frac{k}{Q}, \varphi_1 = 90°, B = 3\gamma Q \text{ and } \varphi_2 = 90°. \tag{8}$$

Substituting (8) into (6) yields what is referred to here as the *broad valley drive signal*,

$$F_{dr} = A\left[\cos(\beta\tau) + B\cos(2\beta\tau)\right], \tag{9}$$

where $A>0$ independently controls the amplitude of the cantilever and $0\leq B<3Q/4$ independently controls the width of the valley.

Remark: The above method can be followed to generate trajectories with narrow valley, also. A narrow valley response results when $-0.25<\gamma\leq 0$, or in terms of the drive signal parameters, $-3Q/4<B\leq 0$. A narrow valley response may be useful when high force is desired, such as in nano-indentation.

In the following we examine, using numerical techniques, the effect of trajectory shape on measurement sensitivity and tip-sample interaction force. Here, measurement sensitivity is defined as the steady-state change in the cantilever trajectory to the change in tip-sample offset. Mathematically this is given by,

$$S = \frac{d}{dx_s} RMS\left(x(t)\right), \tag{10}$$

where *RMS* is the root mean square. The tip-sample interaction force is measured as the average force of the sample on the tip over one period of oscillation, or,

$$\bar{F}_{ts} = \frac{1}{T}\int_T F_{ts}(\tau)\, d\tau, \tag{11}$$

where $T = 2\pi/\beta$ is the period of the trajectory.

III. NUMERICAL ANALYSIS

The following analysis assumes parameters A_1=1.3596x10^{-76} Jm^6, A_2=1.865x10^{-19} J, R= 20 nm, k=7.5 nN/nm, Q=100, and A=1.5 nN corresponding to commercially available antimony doped silicon probe and a silicon substrate. An approach-retract plot

of the cantilever response is shown in Figure 2 with respect to various values of B/Q at resonance (β=1).

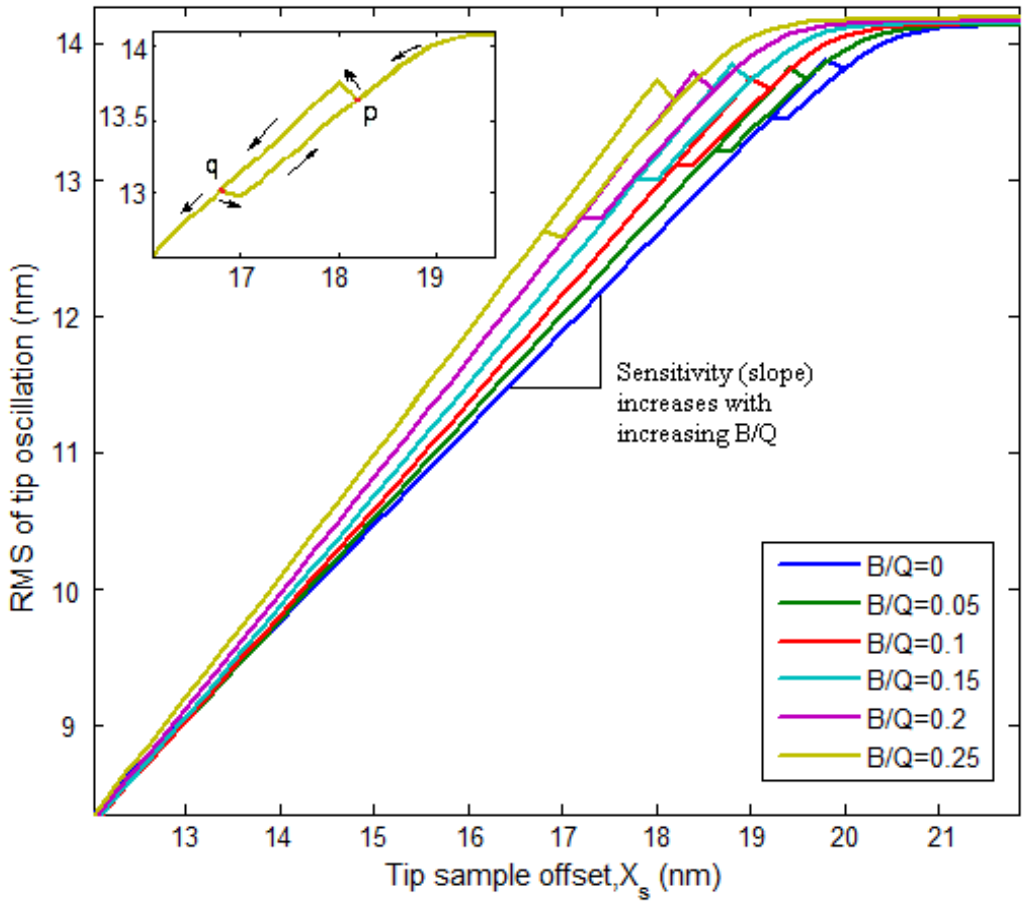

FIG. 2. RMS vs. tip sample offset curves for single harmonic (B/Q=0) and bi- harmonic (B/Q=0.05, 0.1, 0.15, 0.2, and 0.25) drive signals obtained at resonance (β=1). Note: the figure shows the RMS response for both approach and retract phase (inset).

It is well known that AFM tapping dynamics have two stable solutions, which are sometimes referred to as the attractive solution and repulsive solution[29]. The attractive solution is active at large offsets and the repulsive solution is active at small offsets. For a region of offsets in between, both solutions may be active resulting in the hysteretic

loop shown in Figure 2. The hysteretic loop is typically avoided in imaging to prevent the appearance of image artifacts.

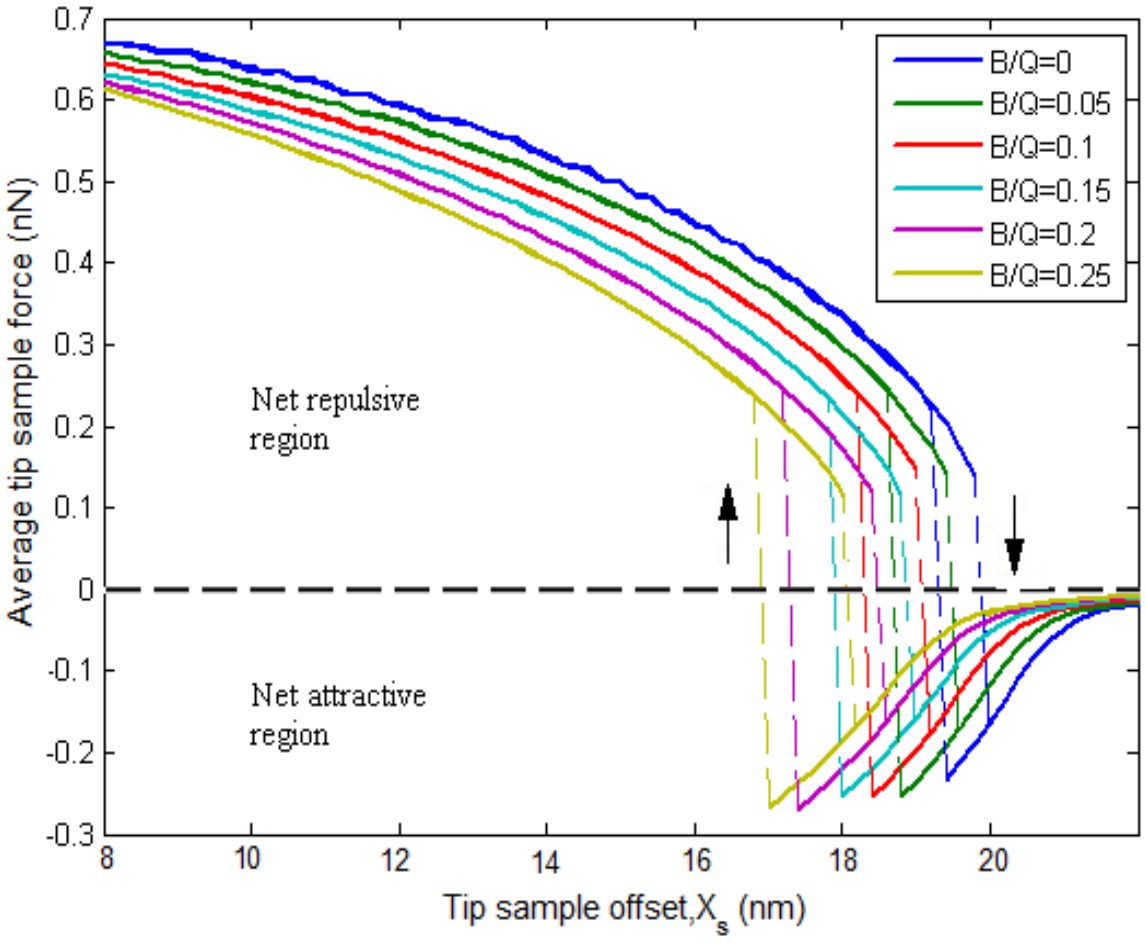

FIG. 3. Average force vs. tip sample offset plot for single harmonic (B/Q=0) and bi harmonic (B/Q=0.05, 0.1, 0.15, 0.2 and 0.25) drive signals. Note: the figure shows the average force for both approach and retract phase.

The measurement sensitivity (10) can be observed as the slope of the approach-retract curve. Imaging typically occurs in the repulsive region, where the slope, and thus measurement sensitivity, is largest and approximately linear. Of particular interest here, is the effect that the bi-harmonic parameter *B* has on the slope in this region, namely a

larger B results in larger measurement sensitivity. The sensitivity for the offset x_s=16 nm is tabulated in Table I. Better than a 30% improvement in measurement sensitivity can be obtained with B=0.25Q compared to B=0, the nominal case with the single harmonic drive signal (3).

TABLE I. Sensitivity measurement at offset x_s= 16 nm

B/Q[a]	**Sensitivity**	**% Increase in sensitivity**
0	0.7076	-
0.05	0.7502	6.02
0.1	0.7918	11.90
0.15	0.8346	17.95
0.2	0.8782	24.11
0.25	0.9215	30.23

[a]B/Q – Ratio of bi harmonic parameter to Q-factor of the cantilever

The average force experienced by the tip during an approach-retract is shown in Figure 3. Solutions in the attractive region have a net attractive force and solutions in the repulse region have a net repulsive force. Notably, the bi-harmonic parameter B has the effect that larger values of B decrease the magnitude of the interaction force. That is, at any offset the net tip-to-sample force is reduced by increasing B. Average repulsive

forces are tabulated in Table II for the offset x_s=16 nm. Using B=0.25Q reduces forces by 34%.

TABLE II. Force measurement at offset x_s= 16 nm

B/Q	Average Force (nN)	% Reduction in average force
0	0.4478	-
0.05	0.4232	5.2
0.1	0.3904	12.8
0.15	0.3595	19.7
0.2	0.3283	26.7
0.25	0.2949	34

IV. EXPERIMENTAL VALIDATION

A Veeco Multi-Mode Scanning Probe Microscope is used in the following experiment. An antimony doped silicon cantilever of resonant frequency, F = 359.7 kHz and quality factor, Q = 350 is used with a silicon sample. The cantilever drive signal generated by the SPM controller was intercepted using a Signal Access Module, and replaced by a bi-harmonic signal generated by a National Instruments digital function generator. The following experiment shows a standard approach-retract curve in which the tip moves towards and away from the sample while the RMS (volts) value of the reflected laser on the optical sensor is recorded. The output was then converted to

nanometers through a suitable conversion factor. Figure 4 shows the resulting curves for several values of *B/Q*. It can be seen that the sensitivity i.e. slope of the curves increase as *B/Q* is increased.

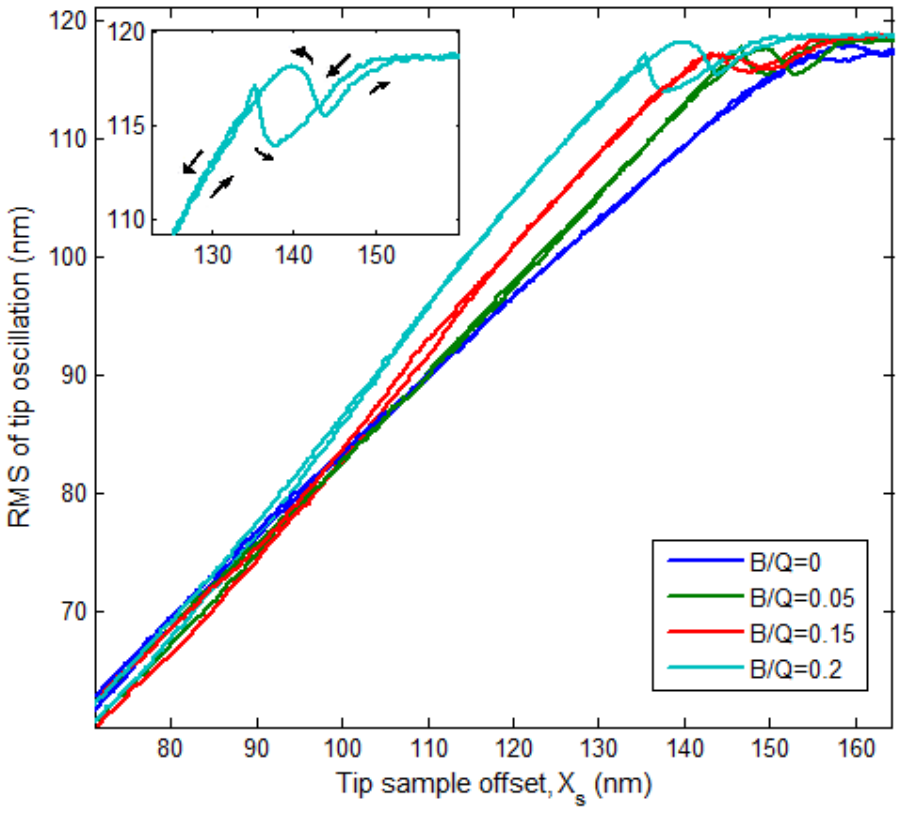

FIG. 4. Experimental *RMS* vs. tip sample offset curves obtained for single harmonic (*B/Q*=0) and bi harmonic (*B/Q*=0.05, 0.15, and 0.2) drive signals. Note: the figure shows the *RMS* response for both approach and retract phase.

Comparing Figure 4 to the numerical study shows similar results. As *B/Q* increases, the slope of the response also increases. That is, for the same change in offset, X_s, there is a greater (and thus more detectable) change in the cantilever trajectory which denotes increase in sensitivity. The sensitivity values were obtained by applying linear least square fit through the data points in the range $80 \leq Xs \leq 130$ nm (linear region) and

measuring the slope. The sensitivities were calculated for each case and are tabulated in Table III.

V. IMPACT ON IMAGING AND TIP WEAR

A. Imaging results Figure 5 shows the obtained images using single harmonic drive (A) and bi-harmonic drive B/Q=0.05 (B) and B/Q=0.1 (C). Fourier transforms of the images in (A), (B), and (C) are shown in (D), (E), (F), respectively. Visual inspection of (A), (B), and (C) clearly shows that the image becomes sharper as B is increased. Sharpness is typically quantified by measuring the high frequency components of the image[30].

TABLE III. Experimental sensitivity measurement obtained through a linear curve fit.

B/Q	Sensitivity	% Increase in sensitivity
0	0.6849	-
0.05	0.7149	4.38
0.15	0.7890	15.19
0.2	0.8252	20.49

To quantify the sharpness improvement, a circle is fit to the spectrum plot whose radius is selected to encompass one half of the spectral content; Results are given in Table IV. The results show that B/Q=0.1 increases the frequency range by about 50% when compared to the single harmonic spatial frequency range.

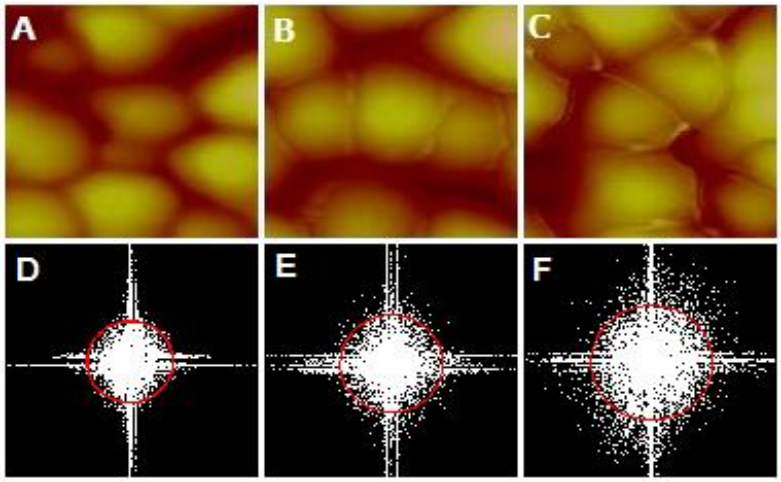

FIG. 5. Images (125 X 125 nm) of BudgetSensors Tip Check sample obtained through single harmonic (A) and bi-harmonic trajectories B/Q=0.05 (B) and B/Q=0.1 (C). Plots (D), (E), (F) represent the spectral content of (A), (B) and (C) respectively.

TABLE IV. Measurement of image sharpness via high frequency radius.

B/Q	**High Frequency Radius (1/pixel)**	**% Increase**
0	0.08550	-
0.05	0.10275	20.17
0.1	0.12404	45.07

B. Tip wear One practical benefit of reducing tip-sample interaction forces is reduction in tip wear. In order to validate low tip-sample interaction forces in bi-harmonic mode, a tip wear test is performed. Two sets of three probes were subjected to wear in single harmonic mode and bi-harmonic mode (B/Q=0.3), respectively. The tips were imaged before and after wear using scanning electron microscope.

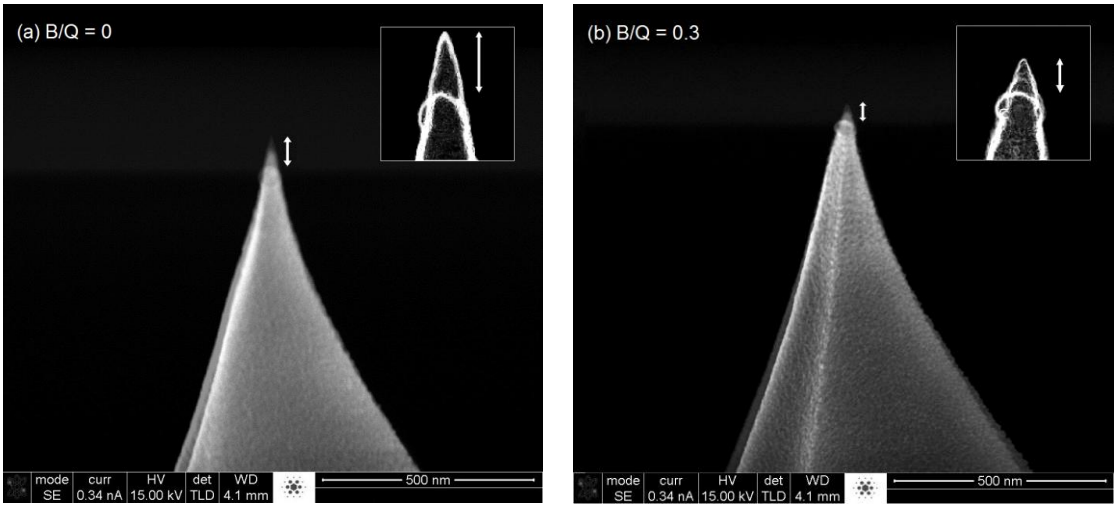

FIG. 6. SEM images of probe tip taken before and after wear test and superimposed to ascertain the loss in tip height (a) Single harmonic mode (b) Bi- harmonic mode (B/Q = 0.3). Insets show the tip images which were filtered using edge detection filter.

TABLE V. Tip height loss measurement

Mode	Probe	Tip height loss (nm)	Mean (nm)
SINGLE HARMONIC	1	55	53
	2	50	
	3	54	
BI-HARMONIC	4	35	34
	5	31	
	6	36	

Figure 6 shows superimposed images of probes subjected to single (Figure 6. *a*) and bi-harmonic mode (Figure 6. *b*), respectively. Both the probes were subjected to 20 image cycles, with each cycle corresponding to 512 scan lines over a 1μm X 1μm area. The wear in the tip was quantified by measuring the loss in tip height from the SEM image. Other tips in the set were also subjected to the same conditions and the loss in tip height was calculated. The results are tabulated in Table V. The mean loss in tip height for bi-harmonic mode is 19 nm less than single harmonic mode. This clearly shows that the wear in the tip subjected to bi-harmonic mode is lesser when compared to that subjected to single harmonic mode.

VI. CONCLUSION

In conclusion, the technique described in this article increases the measurement sensitivity while reducing the tip sample interaction force in AFM tapping mode through the addition of a second harmonic frequency to the drive signal. In the time domain, this can be viewed as altering the probe trajectory from a sinusoidal shape to one that has a broad valley. The broad valley trajectory reduces the velocity of the tip before contact and increases the period of time that the tip spends near the surface, thereby increasing sensitivity to changes in the offset. Experimental results show that the bi-harmonic trajectory yields better resolution at high spatial frequencies and reduced tip wear as compared to single harmonic. Moreover, this technique does not require major configuration changes in TM-AFM instrumentation, which makes it readily deployable.

.

REFERENCES

[1]G. Binnig, C. Quate and C. Gerber, Physical Review Letters **56**, 930 (1986).

[2]Q. Zhong, D. Inniss, K. Kjoller, and V. Elings, Surface Science Letters **290**, L688 (1993).

[3]R. Garcia and A. San Paulo, Physical Review B **66**, 041406 (2002).

[4]T. R. Albrecht, P. Grutter, D. Horne and D. Rugar, Journal of Applied Physics **69**, 668 (1991).

[5]J. Tamayo, A. D. L. Humphris, R. J. Owen, and M. J. Miles, Biophysics Journal **81**, 526 (2001).

[6]T. R. Rodriguez and R. Garcia, Applied Physics. Letters **82**, 4821 (2003).

[7]S. Patil, G. Matei, H. Dong, and P. M. Hoffmanna, Review of Scientific Instruments **76**, 103705 (2005).

[8]T. Fakuma, K. Kobayashi, K. Matsushige and H. Yamadaa, Applied Physics Letters **87**, 034101 (2005).

[9]B. W. Hoogenboom, H. J. Hug Y. Pellmont, S. Martin P. L. T. M. Frederix, D. Fotiadis, and A. Engel, Applied Physics Letters **88**,193109 (2006).

[10]M. Ashhab, M. V. Salapaka, M. Dahleh, and I. Mezi´c, Nonlinear Dynamics **20**, 197 (1999).

[11]A. Sebastian, M. V. Salapaka, D. J. Chen, and J. P. Cleveland, Journal of Applied Physics **89**, 6473 (2001).

[12]R. W. Stark, G. Schitter, and A. Stemmer, Physical Review B **68**, 85401 (2003).

[13]D.R. Sahoo, A. Sebastian and M. V. Salapaka, International Journal of Robust and Nonlinear Controls **15**, 805 (2005).

[14]S.M. Salapaka, T. De, and A. Sebastian, International Journal of Robust and Nonlinear Controls **15**, 821 (2005).

[15]O. Sahin, C.F. Quate, and O. Solgaard, , Physical Review B **69**, 165416 (2004).

[16]O. Sahin, A. Atalar, Applied Physics Letters **79**, 4455 (2001)

[17]R.W. Stark, N. Naujoks, A. Stemmer, Nanotechnology **18**, 065502 (2007).

[18]M. Baumann and R.W.Stark, Ultramicroscopy **110**, 578 (2010).

[19]T. R. Rodriguez and R. Garcia, Applied Physics Letters **84**, 449 (2004).

[20]N.F. Martinez, S. Patil, J. R. Lozano, and R. Garcia, Applied Physics Letters **89**, 153115 (2006).

[21]R.W. Stark, T. Drobek, and W.M. Heckl, Applied Physics Letters **74**, 3296 (1999).

[22]J. R. Lozano and R. Garcia, Physical Review Letters **100**, 076102 (2008).

[23]R. Proksch, Applied Physics Letters **89**, 113121 (2006).

[24]M. Balantekin and A. Atalar, Applied Physics Letters **87**, 243513 (2005).

[25]J. Israelachvili, *Intermolecular and Surface Forces*, Academic Press, Boston, MA, 1985.

[26]S. Rützel, S.I. Lee and A. Raman, Proceedings of the Royal Society **459**, 1925 (2002).

[27]N. Jalili and K. Laxminarayana, Mechatronics **14**, 907 (2004).

[28]J. Legleiter, Nanotechnology **20** (2009).

[29]A. Sebastian, A. Gannapalli and M. V. Salapaka, IEEE Transactions on Control System Technology **15**, 952 (2007).

[30]M.T. Postek and A.E. Vladár, Scanning **20**, 1 (1998).

II. BI-HARMONIC CANTILEVER DESIGN FOR IMPROVED MEASUREMENT SENSITIVITY IN TAPPING-MODE ATOMIC FORCE MICROSCOPY

Muthukumaran Loganathan and Douglas A Bristow

ABSTRACT

We report the development of bi-harmonic cantilevers, a set of cantilevers whose second resonant frequency is twice its first resonant frequency, for tapping-mode AFM operation. Such cantilevers exhibit improvement in measurement sensitivity when tapped with an oscillating trajectory whose valleys are broader compared to conventional sinusoidal trajectory. Broad valley tapping trajectories can be generated using drive signals composed of two harmonics which are in this case the first two flexural modes of the cantilever. Matching the harmonics of the drive signal with the flexural modes enables trajectory shaping to be achieved with relatively small drive force. Numerical simulations show that bi-harmonic cantilevers provide better sensitivity without saturating the input drive signal. We also present the actual mechanical design and working of such a cantilever. Experimental results obtained with the bi-harmonic cantilevers indicate improved surface tracking which is a direct benefit of higher sensitivity.

1. INTRODUCTION

Conventional Tapping-mode AFM [1] involves exciting a micro cantilever with a nano sized tip near its resonant frequency and tapping the surface of interest intermittently. The surface variations are recorded by regulating the amplitude of the

trajectory through a feedback loop and monitoring the feedback signal. This method has been successfully used to image variety of samples including conductive, non-conductive and biological samples over various imaging conditions.

Though the steady state tapping trajectory is predominantly sinusoidal with the frequency same as the driving signal, it does contain higher harmonic components [2-4] purely due to non-linear tip sample interaction. Since non linear surface forces are characteristic of the material, variations in higher harmonics can be directly correlated to surface inhomogeneities [5-7]. Apart from material contrast, higher harmonic imaging was used to map electrostatic forces [8-9]. Though higher harmonics contain valuable information, the poor signal-to-noise ratio at the corresponding frequencies makes measurements inaccurate. This led to the idea of redesigning cantilevers to have one of the higher eigenmode an integer multiple of the fundamental resonant mode [10]. Such an approach improved the signal to noise ratio and made the harmonics sensitive to surface properties. Apart from single eigenmode excitation, significant compositional sensitivity was also achieved by driving the cantilever with multi-frequency signals. Garcia et al proposed a method to obtain compositional maps by exciting first two modes of the cantilever [11-12] and monitoring the phase of the second eigenmode.

The concept of multi frequency drive signals was not only used to obtain material maps but was also employed to improve the measurement sensitivity of the AFM. The measurement sensitivity was improved by tapping the cantilever with a broad valley trajectory [13] which can be generated by driving the cantilever with a drive signal composed of two harmonics. However, since the rectangular cantilever does not readily

respond to second harmonic of the drive signal large input voltage has to be fed in to reshape the trajectory.

In this article, we overcome the above disadvantage by proposing a new cantilever design whose second mode frequency is twice its first mode. Such a cantilever has high amplification at first and second harmonic frequency and hence can be readily made to tap with a broad valley trajectory without saturating the input drive signal. Henceforth, these types of cantilever will be designated as bi-harmonic cantilevers. We also show how the measurement sensitivity can be improved with least modifications to the cantilever geometry.

2. MODEL DESCRIPTION

A broad valley trajectory, as shown in figure 1, is a trajectory whose valley is broader compared to a sinusoidal tapping trajectory. One possible representation of a broad valley trajectory is,

$$z_{desired}(t) = A_0\left[\cos(\omega t) + \gamma\cos(2\omega t)\right], \tag{1}$$

Where, A_0 controls the amplitude and $0 \le \gamma \le 0.25$ controls the width of the valley of the trajectory. Considering the cantilever as a lumped mass system, a trajectory as in eqn (1) can be generated by driving the system with an input force signal composed of two harmonics. The broad valley trajectory can be achieved with less input force if the cantilever system has two resonant modes matching the two harmonics of the broad valley trajectory. In other words, if a cantilever has a second resonant frequency twice

that of its first resonant frequency it can be effectively used to reshape the tapping trajectory with less input force.

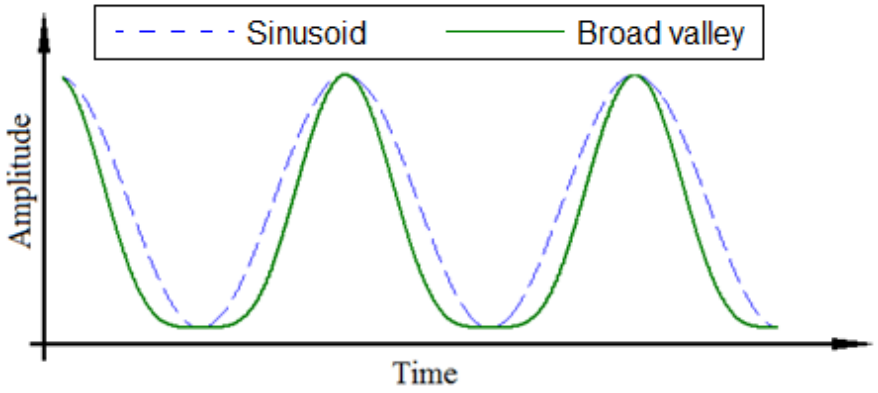

Figure 1. Comparison of sinusoidal and broad valley trajectories

Assuming the dynamics are mostly contained in the first two resonant modes, such a cantilever can be modeled as a system of two 2nd order differential equations [14], one for each resonant mode of the cantilever. Now considering the system is operated at 1st resonance, the model can be represented as,

$$\begin{aligned} m_1\ddot{z}_1 &= -k_1 z_1 - \frac{m_1\omega_1}{Q_1}\dot{z}_1 + F_{dr}(t) + F_{ts}(z_1 + z_2) \\ m_2\ddot{z}_2 &= -k_2 z_2 - \frac{m_2\omega_2}{Q_2}\dot{z}_2 + F_{dr}(t) + F_{ts}(z_1 + z_2) \end{aligned} \tag{2}$$

where, m_i, k_i, Q_i, and ω_i are the effective mass, stiffness, Q-factor, and angular frequency of the i^{th} eigenmode. For the cantilever under consideration, $\omega_2 = 2\omega_1$. In order to generate a trajectory that contains two harmonics (eqn. 1) an input drive signal composed of two harmonics is required. Hence drive signal F_{dr} can be represented as,

$$F_{dr}(t) = F_1\cos(\omega_1 t - \theta_1) + F_2\cos(\omega_2 t - \theta_2), \tag{3}$$

where, F_i and θ_i are the drive force and phase shift applied at i^{th} harmonic. Fts is the non linear tip-sample interaction force. The total displacement of the tip from its equilibrium can be written as,

$$\begin{aligned} z(t) &= z_1(t) + z_2(t) + O(\varepsilon) \\ &\approx A_1 \cos(\omega_1 t - \phi_1) + A_2 \cos(\omega_2 t - \phi_2), \end{aligned} \tag{4}$$

where A_i and φ_i are the Amplitude and phase difference of the i^{th} eigenmode. $O(\varepsilon)$ represents the contributions of higher harmonics and eigenmodes. Here, we use the Lennard-Jones [15] potential to model the non-linear interaction,

$$\mathrm{F}_{ts}\left(x\right) = \frac{H_1 R}{180\left(x_s + z\right)^8} - \frac{H_2 R}{6\left(x_s + z\right)^2}, \tag{5}$$

where, A_1 and A_2 are the repulsive and attractive Hamaker constants respectively. R is the probe tip radius and x_s is the distance between the cantilever equilibrium and sample. The free response of the cantilever can be shaped to have the desired broad valley trajectory by carefully selecting parameters F_i and θ_i, which can be obtained through standard Fourier analysis. They are,

$$F_1 = A_0 \frac{k_1}{Q_1}, \quad \theta_1 = -90^\circ, \quad F_2 = \frac{k_2}{Q_2}\gamma A_0, \quad \theta_2 = -90^\circ. \tag{6}$$

Substituting (5) in (3) gives what will be referred here as bi harmonic drive signal,

$$F_{dr}(t) = F_1 \cos(\omega_1 t + \pi/2) + F_2 \cos(2\omega_1 t + \pi/2). \tag{7}$$

3. BI-HARMONIC CANTILEVER THEORY

Consider a hard surface being tapped in air. The tip surface force profile, for such a scenario, can be approximated to be an impulse function. It is also known that an impulse function contains infinite harmonics, and can written as,

$$\begin{aligned} F_{ts} &\approx \delta(\omega_1 t - \omega_1 t_0) \\ &\approx f_{ts}\cos(\omega_1 t - \omega_1 t_0) + f_{ts}\cos(\omega_2 t - \omega_2 t_0) + ..., \end{aligned} \tag{8}$$

Where, f_{ts} is the average energy of the force function and t_0 is the time when the cantilever comes in contact with the surface. Since the system attenuates all inputs except those that match the 1st and 2nd resonant modes, the model equivalent to eqn (2) can be represented as,

$$\begin{aligned} m_1\ddot{z}_1 &= -k_1 z_1 - \frac{m_1\omega_1}{Q_1}\dot{z}_1 + F_{dr}(t) + f_{ts}\cos(\omega_1 t - \omega_1 t_0) \\ m_2\ddot{z}_2 &= -k_2 z_2 - \frac{m_2\omega_2}{Q_2}\dot{z}_2 + F_{dr}(t) + f_{ts}\cos(\omega_2 t - \omega_2 t_0) \end{aligned} \tag{9}$$

Where $\omega_2 = 2\omega_1$. The output z_1 can be written as,

$$z_1(t) = A_1 e^{j\phi_1} = G_1(j\omega_1)\left[F_1 e^{-j\theta_1} + f_{ts}e^{-j\omega_1 t_0}\right], \tag{10}$$

Where, G_1 is the transfer function representation of the 1st mode of the cantilever and is given by,

$$G_1(s) = \frac{\omega_1^2 / k_1}{s^2 + \frac{1}{Q_1}s + \omega_1^2}. \tag{11}$$

By making the 2nd mode of the cantilever stiffer than the 1st mode, the effect of tip surface forces on 2nd mode deflection z_2 can be made small. z_2 can be represented as,

$$z_2(t) = A_2 e^{j\phi_2} = G_2(j\omega_2)\left[F_2 e^{-j\theta_2} + f_{ts} e^{-j\omega_2 t_0}\right] \approx G_2(j\omega_2)\left[F_2 e^{-j\theta_2}\right]. \quad (12)$$

From eqn (11), it can be inferred that by making the 2nd mode stiffer parameters A_2 and ϕ_2 can be made independent of the tip offset and hence, can be held constant for all interactions (A_{2c} and ϕ_{2c}). From (9) the surface force can written as,

$$f_{ts} e^{-j\omega_1 t_0} = \frac{A_1 e^{j\phi_1}}{H_1(j\omega_1)} - F_1 e^{-j\theta_1}. \quad (13)$$

By setting A_1 to be a particular value A_{1c} we can calculate F_1 for a given system H_1. θ_1 and θ_2 are chosen from (5) corresponding to broad valley trajectory. The unknown parameters in eqn (12) are f_{ts}, t_0 and ϕ_1. From the infinite solutions (z_1) that can be generated from the combination of A_1 and $\phi_1=(0,2\pi)$ there is only one solution whose time of impact (t_0) that satisfies eqn (12). Let the ϕ_1 corresponding to this valid solution be ϕ_{1c}. Thus the valid tapping trajectory for any given A_{1c} and A_{2c} can be written as,

$$z_{tapping}(t) = A_{1c}\left[\cos(\omega_1 t - \phi_{1c}) + \gamma \cos(2\omega_1 t - \phi_{2c})\right], \quad (14)$$

where, $\gamma = A_{2c}/A_{1c}$. Since, the analysis pertains to hard samples the lowest point on the trajectory in eqn (13) can be considered as the location of the sample surface. That is,

$$Tip\,offset,\ x_S = \left|\min(z(t))\right|. \quad (15)$$

The measurement sensitivity of the cantilever is defined as the change in root mean square (RMS) of the trajectory to the change in tip sample offset

$$S = \frac{d}{dx_S} RMS\left(z(t)\right), \tag{16}$$

The RMS of eqn (14) is plotted for every tip offset (x_s) as in eqn (15) for both single harmonic (A_2=0) and bi-harmonic trajectories (γ=A2/A_1=0.2) along with the respective simulation curves in figure 2.

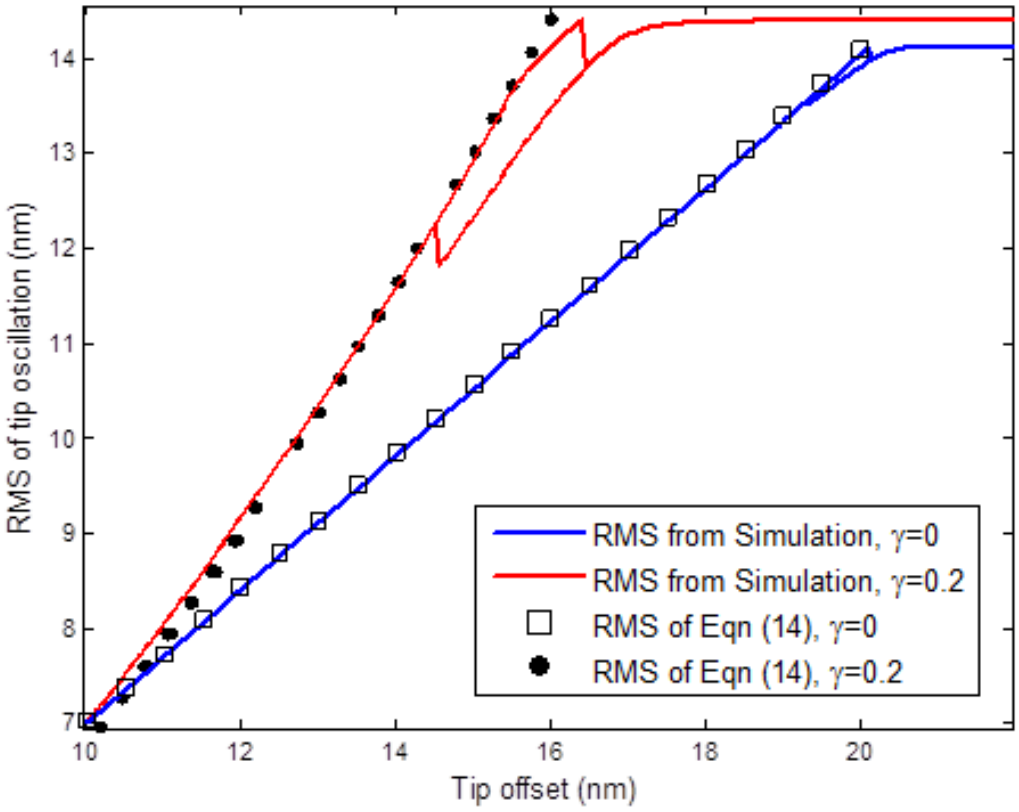

Figure 2. *RMS* vs. tip sample offset (x_s) obtained through analytical framework and numerical simulation for single harmonic (γ=0) and bi-harmonic (γ= 0.2) trajectories.

Figure 2 shows the agreement between analytical and simulation sensitivity improvement, which can be obtained, provided the surface under consideration is a hard surface and the 2nd mode of the cantilever is lot stiffer compared to the 1st mode. The 2nd

assumption can be achieved by designing the bi-harmonic cantilever to satisfy the criteria.

4. NUMERICAL ANALYSIS

The model described in section 2 was analyzed using numerical technique to estimate the measurement sensitivity of the cantilever. The system parameters were chosen by performing a model fit to the frequency spectrum of the finite element model of the bi-harmonic cantilever (figure 6(a)). The parameters are k1=15 nN/nm, k2=1355.2 nN/nm, Q1=100, Q2=300, ω1=200 kHz, ω2=400 kHz.

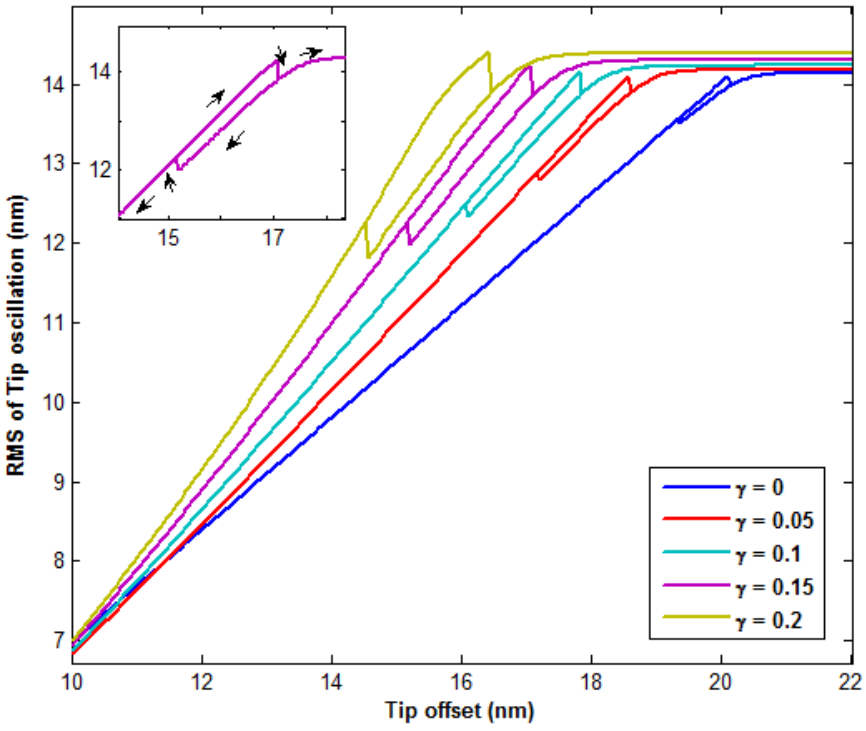

Figure 3. *RMS* vs. tip sample offset (x_s) of bi-harmonic cantilever for single harmonic (γ=0) and bi-harmonic (γ=0.05, 0.1, 0.15, 0.2) obtained at ω_1=200 kHz and ω_2=400 kHz. Inset shows the approach and retract direction.

From eqn (16) it can be seen that measurement sensitivity is the slope of the approach retract curve shown in figure 3. It is interesting to note that tapping both regular and bi-harmonic cantilever with a single harmonic drive signal yield same sensitivity value of 0.707[10]. Hence this can be used as point of comparison to evaluate the sensitivity improvement. As γ is increased i.e. as the width of the broad valley is increased the measurement sensitivity also increases. Table 1 tabulates the sensitivity obtained for different values of γ at tip offset of x_s=13 nm. More than 70% improvement in sensitivity is observed with γ=0.2 compared to single harmonic tapping (γ=0). Not only has the sensitivity improved but the input force (F_2) at second mode is small compared to bi-harmonic operation using regular cantilever [10]. This, from the instrumentation side means that bi-harmonic cantilever can be made to tap with broad valley without saturating the input drive signal. It can also be noted that increasing γ has reduced the effective operating range of the cantilever, however this can be recovered by tapping with larger amplitude while preserving the higher sensitivity.

TABLE 1. Sensitivity measurement at x_s= 13 nm

γ	**F_2 (nN)**	**Sensitivity**	**% Increase**
0	0	0.707	-
0.05	4.47	0.841	18.95
0.1	8.95	0.931	31.6
0.15	13.4	1.05	48.51
0.2	17.9	1.22	72.56

5. CANTILEVER DESIGN

For nominal rectangular cantilevers the second resonant frequency is normally greater than twice its first resonant frequency ($\omega_2 >> 2\omega_1$). Hence, in order to match the second resonant mode to the second harmonic, it has to be reduced without affecting the fundamental resonant frequency. Resonant frequencies of rectangular cantilever can be varied by selectively removing material from high stress location corresponding to that mode [16-17]. This reduces the effective spring constant of that mode which in turn reduces the frequency of the mode.

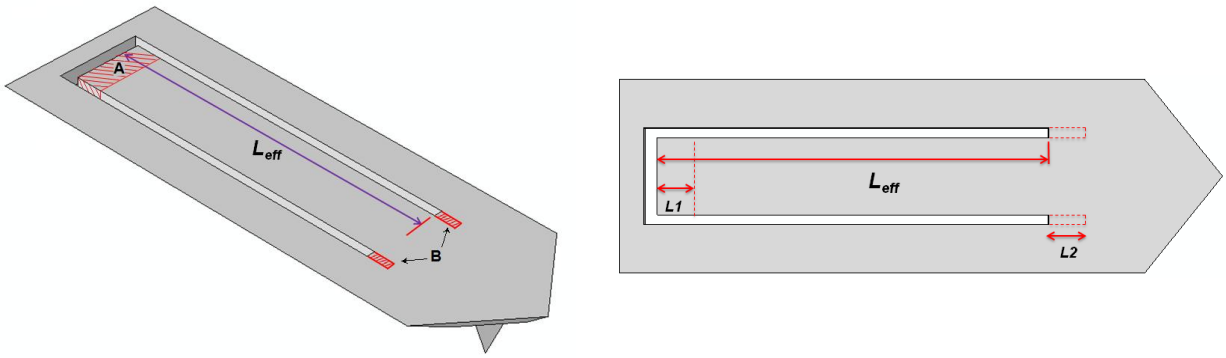

(a) (b)

Figure 4. (a) Bi-harmonic Cantilever setup (b) Top view of the cantilever showing dimensions that can be altered (L_1, L_2) to tune the 2nd mode of the cantilever.

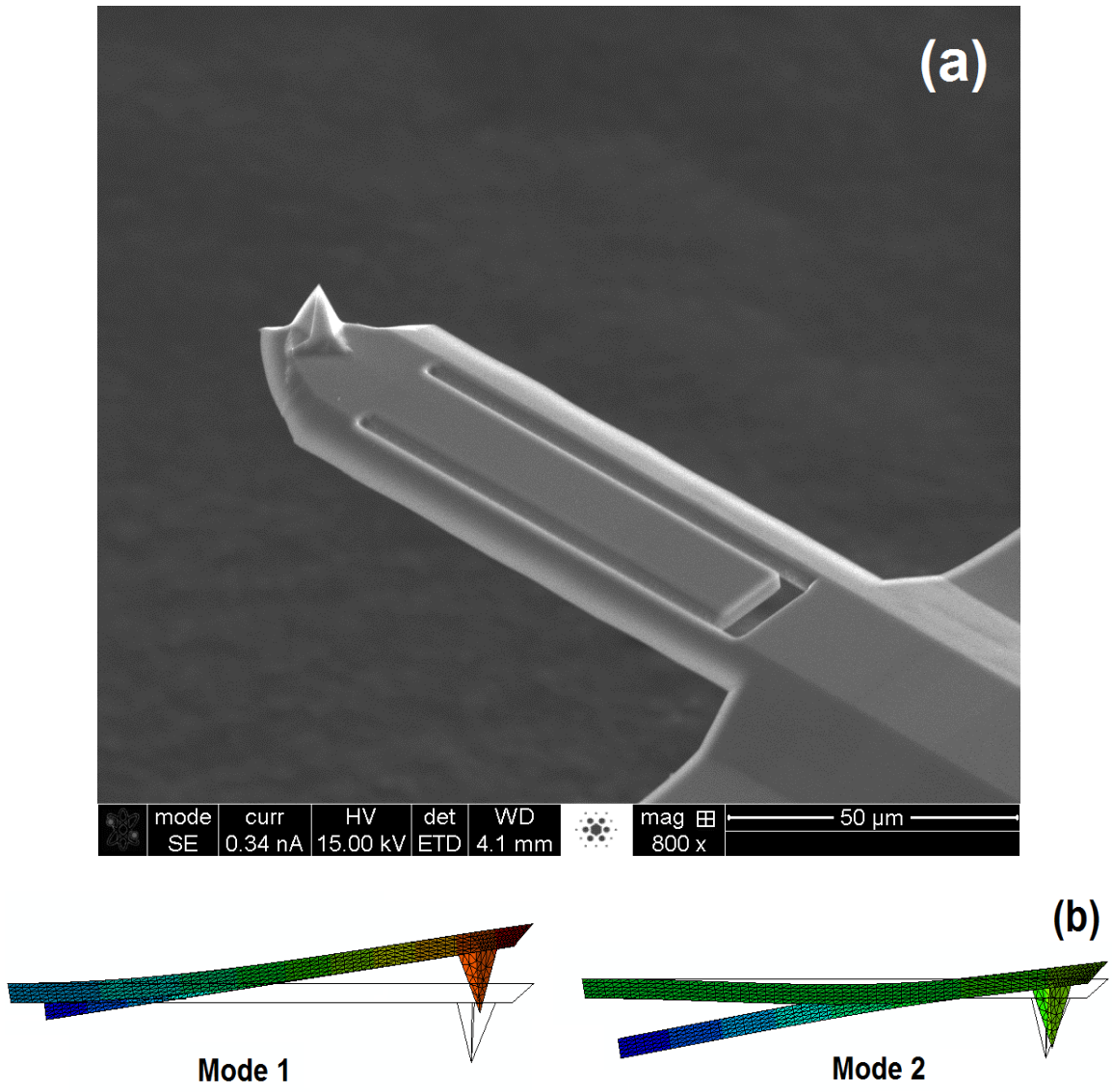

Figure 5. (a) SEM image of bi-harmonic cantilever fabricated using Focused Ion Beam (FIB). (b) First and second resonant mode shape of the cantilever with a fixed base and free end (tip). The resonant frequencies are 200 kHz and 400 kHz respectively.

The proposed cantilever as shown in figure 4 has an inner beam that oscillates freely. Such a design reduces the 2^{nd} mode frequency yet maintains a relatively higher 2^{nd} mode stiffness (k_2=1355.2 nN/nm) compared to the 1^{st} mode (k_1=15 nN/nm). Figure 5(a) shows the bi-harmonic cantilever fabricated from commercial silicon cantilever (TESP)

manufactured by BRUKER FEI Helios NanoLab 600 focused ion beam (FIB) was used for etching. The unmodified cantilever was 125 μm long, 40 μm wide and 4 μm thick. The bi-harmonic cantilever has an inner beam of 84 μm in length and 16 μm in width. The dimensions of the inner cantilever were narrowed upon using dynamic analysis performed through finite element technique. Figure 5(b) shows the mode shapes of the cantilever at the first and second resonant mode.

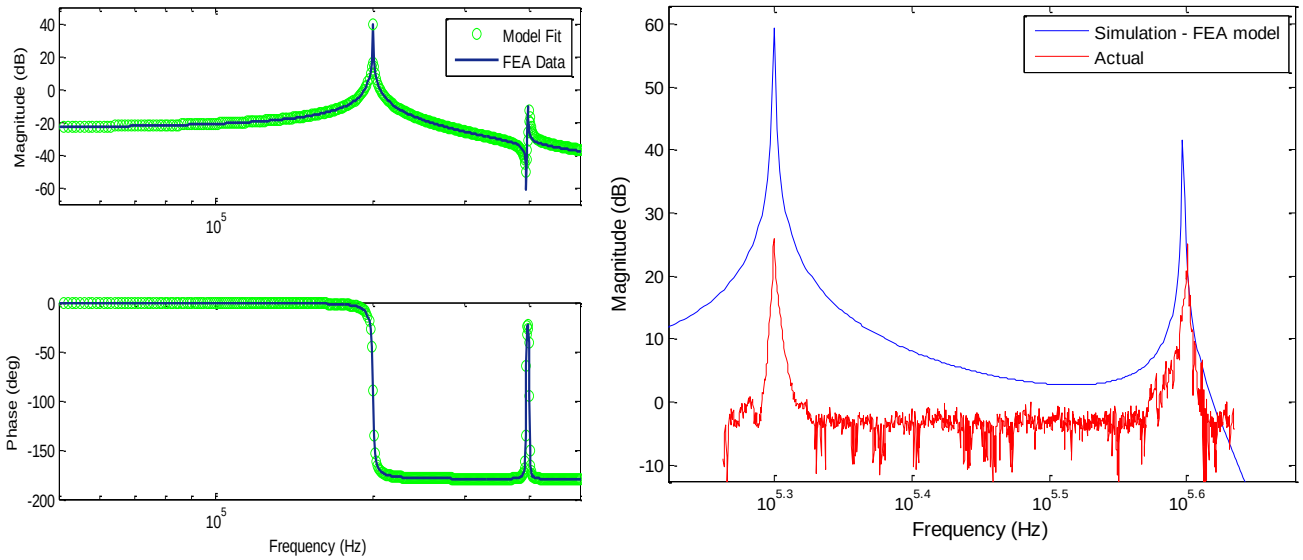

Figure 6. (a) Frequency spectrum of bi-harmonic cantilever (force input) obtained through finite element analysis. (b) Frequency response of fabricated bi-harmonic cantilever (base motion input) shown in Figure 5.

The frequency spectrum of the finite element model and the fabricated cantilever are shown in figure 6(b). This design is not only simple but also provides ways to retune the 2nd mode frequency. Normally resonant frequencies of the fabricated cantilever may not exactly match the simulation due to uncertainties in cantilever material properties and fabrication errors. In such cases the frequency deviation can be corrected by modifying

the effective length (L_{eff}) of inner beam suitably. Increasing the effective length of the inner beam decreases the second resonant frequency and vice versa, without much affecting the first mode. The length of the inner beam can be decreased or increased by removing material corresponding to region L_1 or L_2 respectively.

6. EXPERIMENTAL VALIDATION

Experiments were carried out on a Veeco Multi-Mode scanning probe microscope. The bi-harmonic cantilever was made to scan a cobalt sample. The default sinusoidal drive signal was replaced by bi-harmonic drive signal generated by National Instruments digital function generator. The experiment was setup such that the sample approaches and retracts from the tip at a constant rate, and the RMS (volts) value of the reflected laser signal from the photo detector was recorded.

The experimental sensitivity was calculated by measuring the slope of the linear region ($60 \leq x_s \leq 100$ nm) of the experimental data shown in figure 7. The sensitivity improvement was about 33% compared to single harmonic tapping. The experimental sensitivity improvement is lower than that estimated in simulation because it depends on both tip radius and stiffness which are uncertain parameters due to tip wear and fabrication errors respectively.

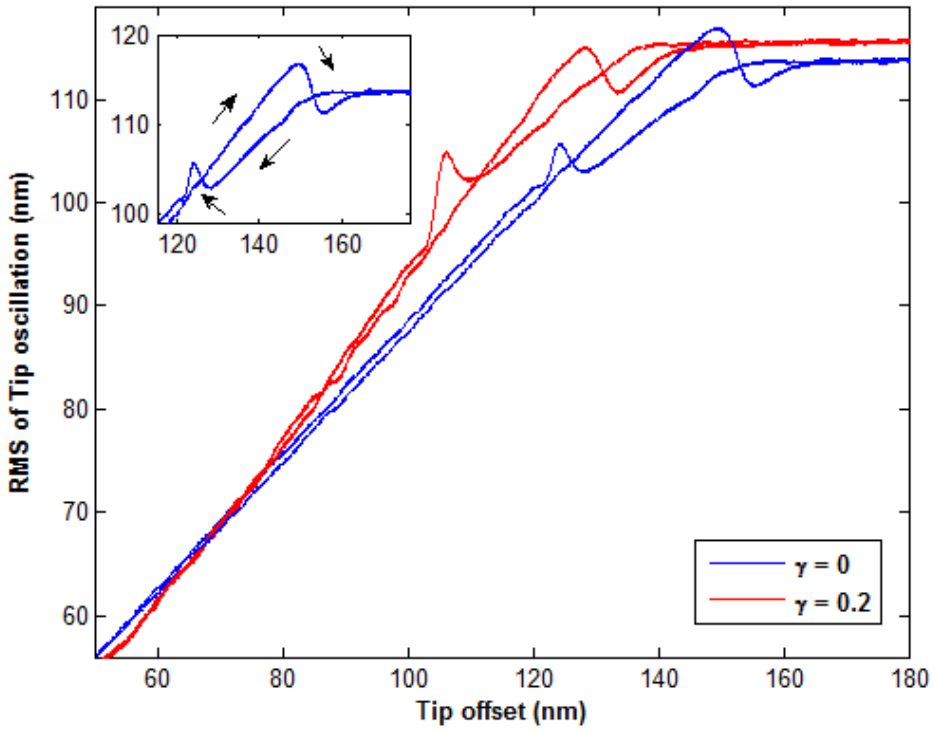

Figure 7. Experimental *RMS* vs. tip sample offset curves of bi-harmonic cantilevers corresponding to single harmonic (γ=0) and bi-harmonic (γ= 0.2) trajectory. Inset shows the approach and retract direction.

The real benefit of improvement in sensitivity can be seen in figure 8. The tapping trajectory was changed from single to bi-harmonic half way through the scan while the controller gains were kept constant. In Single harmonic operation the error signal (figure 8(a)) was considerably small which resulted in poor surface height tracking (figure 8(b)). When the trajectory was switched to bi-harmonic, due to increase in sensitivity of the cantilever the error signal was relatively large which lead to good surface tracking and improved image sharpness.

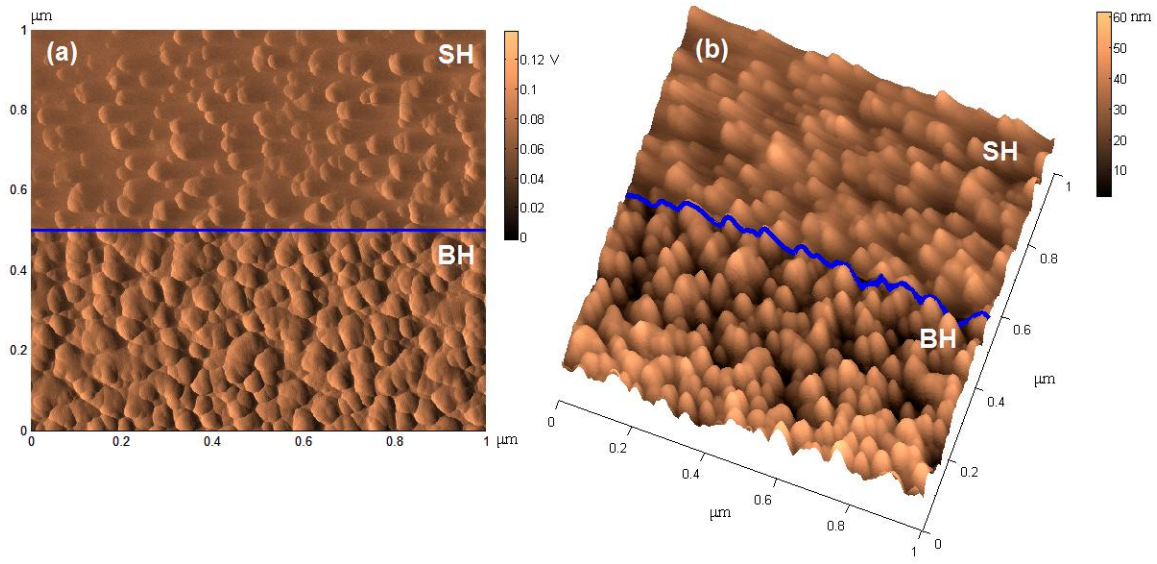

Figure 8. Cobalt sample 1 X 1 µm scan. (a) Absolute amplitude error (b) Three dimensional topography. Note: SH indicates single harmonic tapping and BH indicates bi-harmonic tapping.

7. CONCLUSION

In conclusion, to overcome the difficulty in reshaping the tip trajectory to have a broad valley we have developed a cantilever whose second resonance is twice its first resonance. This cantilever readily responds to bi-harmonic drive signals which are used to obtain broad valley trajectory. Experimental results indicate improved measurement sensitivity and imaging results corroborate numerical and experimental results by exhibiting improved surface tracking.

REFERENCES

[1] Binnig G, Quate C and Gerber C 1986 Physical Review Letters **56**, 1986, 930-3

[2] Stark M, Stark R W, Heckl W M and Guckenberger R 2000 Applied Physics Letters **77** 3293-95.

[3] Tamayo J 1999 Applied Physics Letters **75** 3569-71

[4] Stark R W and Heckl W M 2000 Surface Science **457** 219-28

[5] Hillenbrand R, Stark M and Guckenberger R 2000 Applied Physics Letters **76** 3478-80

[6] Stark R W and Heckl W M 2003 Review of Scientific Instruments **74** 5111-4

[7] Stark R W, Drobek T and Heckl W M 1999 Applied Physics Letters **74** 3296-8

[8] Van Noort S J T, Willemsen O H, Van der Werf K O, de Grooth B G and Greve J 1999 Langmuir **15** 7101-7

[9] Stark R W, Naujoks N and Stemmer A 2007 Nanotechnology **18** 065502-7

[10] Sahin O, Quate C F, Solgaard O and Atalar A 2004 Physical Review B **69** 165416-9

[11] Rodríguez T R and García R 2004 Applied Physics Letters **84** 449-451

[12] Martinez N F, Patil S, Lozano J R and Garcia R 2006 Applied Physics Letters **89** 153115-3

[13] Loganathan M, Kodandarama S R and Bristow D A 2011 Review Scientific Instruments **82** 103704-5

[14] Lozano J R and Garcia R 2008 Physics Review Letters **100** 076102-4

[15] J. Israelachvili, *Intermolecular and Surface Forces*, Academic Press, Boston, MA, 1985

[16] Sahin O, Yaralioglu G, Grow R, Zappe S F, Atalar A, Quate C, Solgaard O 2004 Sensors and Actuators A **114** 183-90

[17] Felts J R and King W P 2009 Journal of Micromechanics and Microengineering **19** 115008-6

SECTION
3. CONCLUSION

This thesis addresses the task of improving the sensitivity of tapping mode (TM) atomic force microscope. A novel method of improving the sensitivity through tip trajectory reshaping has been proposed, described, simulated and experimentally validated. Practical benefits of implementing this method include sharper surface images, reduced tip wear, readily deployable without much configuration changes to the existing AFM. Trajectory shaping involves tapping with a broad valley trajectory that can be obtained by adding a second harmonic component to the regular sinusoidal drive signal. It was observed that the measurement sensitivity improved as the width of the broad valley was increased by increasing the second harmonic amplitude of the drive signal. Hence, higher second harmonic drive amplitude is desired. However, the power constraint on the electric hardware (saturation) poses a limit on the maximum amplitude achievable. Moreover due to cantilever's poor gain at the second harmonic large drive second harmonic signals are required to obtain a reasonable broad valley shaping.

In order to overcome this problem, a new cantilever design whose second resonant frequency is twice its first resonant frequency was proposed. Such a cantilever has good gains at both first and second harmonic frequencies (provided the cantilever is operated at its resonance). Simulation demonstrates improved sensitivity obtained with relatively small second drive amplitude. The bi harmonic cantilever, owing to the simplicity of the design, can be easily implemented on commercially available AFM cantilevers with very less geometrical change. Experimental results show improved surface tracking which is a direct indication of improved sensitivity. This sensitivity improvement method can also be effectively extended to non contact AFM.

APPENDIX
MATLAB PROGRAMS

A.1 PROGRAM TO OBTAIN APPROACH-RETRACT SIMULTION CURVES

```
clc;
clear all;
w1=2*pi*200e3;
w2=2*pi*400e3;
k1=15;
k2=1355.2;
Q1=100;
Q2=300;
x0=[0 0 0 0];
a1=[0 1;-w1^2 -w1/Q1];
a2=[0 1;-w2^2 -w2/Q2];
b1=[0 w1^2/k1]';
b2=[0 w2^2/k2]';
c1=[1 0];
c2=[1 0];
beta=200000*2*pi;
AA=blkdiag(a1,a2);
BB=[b1;b2];
CC=[1 0 1 0];
DD=0;
Cobs=eye(4);
Dobs=zeros(4,1);

sys=ss(AA,BB,CC,DD);

% Tip force parameters
H1=1.3596e-76;                          % Hamaker repulsion constant(Jm^6)
H2=1.865e-19;                           % Hamaker attraction constant(J)
R=20e-9;                                %Tip Radius(m)

% For Input initial conditions
A0=0;
B=0;                                    % 2nd harmonic amplitude
A=3e-9;                                 % 20nm drive amplitude

XX=zeros(2501,1);
convergence_epsilon = 1e-11;

% Tip offset sweep
xs_v =1e-9*[22:-0.05:6 6.05:0.05:22];  % Sweep Up
    peak_to_peak = 0;
    Average_Force=0;
    peak_force=0;
       for i=1:length(xs_v)
       xs = xs_v(i);
       display(sprintf('Calculating response for xs = %d',xs))
       flag_converged=0;
       max_history = 0;
```

```
        min_history = 0;
        run_number=0;
        force=0;
         rms=0;
         con_num=0;
         Y=0;
         while(~flag_converged)
            sim('Garcia_sim',2*pi/beta);    % Simulink program call
             run_number = run_number + 1;
             max_history(run_number) = max(x);
             min_history(run_number) = min(x);
             force(run_number) = max(Fts);

             % check convergence
if (run_number > 100)
   if (norm((max_history(run_number-99:run_number)-
max_history(run_number)),2) < convergence_epsilon) || run_number > 4000
       if (norm((min_history(run_number-99:run_number)-
min_history(run_number)),2) < convergence_epsilon) || run_number > 2000

               rms = sqrt(sum(x.^2)/length(x));
               bc=xf;
               con_num=con_num+1;
               if (con_num == 1)
                   XX=horzcat(XX,x);
                   flag_converged = 1;
               end
               end
               end
             end
if (mod(run_number,100)==0); display(sprintf('Running period
%i',run_number)); end;
         x0=xf';
         end

peak_to_peak(i) = (max_history(run_number) -
min_history(run_number))/2;
vtip(i)=virial_tip;
display(sprintf(' xs = %d completed',xs))
Average_Force(i)=Favg/2/pi/beta;
peak_force(i) = force(run_number);
RMS(i)=rms;
end

display(sprintf('AMPLITUDE'));
num2str(peak_to_peak', '%4.5e\n')
display(sprintf('RMS'));
num2str(RMS', '%4.5e\n')
```

A.2 PROGRAM TO MEASURE HIGH FREQUENCY CONTENT OF AN AFM IMAGE

```
% Image Processing to get the 2D - Fourier Transform
clear all;
clc;
format long;

img_r=imread('img_bq0.1.jpg');    % Image to be analyzed
thres=8.75;                        % threshold value

img=double(rgb2gray(img_r))+1;
nor=size(img);

U=-0.5:1/nor(1):0.5-1/nor(1);
V=-0.5:1/nor(2):0.5-1/nor(2);

% 2D FOURIER TRANSFORM OF THE IMAGE
IMG_F=fft2(img);
IMG_F=fftshift(IMG_F);
a=abs(IMG_F);
Z=log(1+abs(IMG_F));

% THRESHOLDING OF THE FOURIER SPECTRUM
count=0;
for i=1:nor(1)
    for j=1:nor(2)
        if Z(i,j)<=thres
            Z(i,j)=0;
        else
            Z(i,j)=1;
             count=count+1;
             dist(count)=(sqrt((U(i)^2)+(V(j)^2)));
        end
    end
end

radius=mean(dist);

% PLOT THE 50% CIRCLE FIT
for i=1:nor(1)
    for j=1:nor(2)
if abs(U(i)^2)+(V(j)^2 - (radius)^2) < 0.001 && abs(U(i)^2)+(V(j)^2 -
                                                    (radius)^2) > 0.00001
            circ(i,j)=1;
        else
            circ(i,j)=0;
        end
    end

end
circ_3(:,:,1)=circ;circ_3(:,:,2)=circ*0;circ_3(:,:,3)=circ*0;
Z_3(:,:,1)=Z-circ;Z_3(:,:,2)=Z-circ;Z_3(:,:,3)=Z-circ;
figure;imshow(uint8(255.*(2.*circ_3+Z_3)));
fprintf('%10.5f \n',radius);
```

VITA

Muthukumaran Loganathan was born in Tamil Nadu, India. He obtained his bachelor degree in Mechanical Engineering (University rank: 27/2022) on May 2010 from Rajalakshmi Engineering College, which is affiliated to Anna University, Tamil Nadu, India.

He joined Missouri University of Science and Technology in fall 2010 to pursue Masters in Mechanical Engineering with specialization in Control Systems. He worked in the Precision Motion Control lab (PMCL) at Missouri S&T under Dr. Douglas Bristow. He received his Master of Science degree in Mechanical Engineering in December 2012.